

The influence of platinum on UV and ‘visible’ photocatalysis by rutile and Degussa P25

Terry A. Egerton*, John A. Mattinson

*School of Chemical Engineering & Advanced Materials, University of Newcastle Upon Tyne,
Newcastle upon Tyne NE1 7RU, UK*

Received 17 April 2007; received in revised form 23 August 2007; accepted 24 August 2007
Available online 30 August 2007

Abstract

The influence of platinum on the UV photocatalytic degradation of dichloroacetate anion (DCA) by a high area rutile and by the, mainly anatase, P25 form of TiO_2 has been compared. Platinum was deposited photochemically and Pt(II) was generally more active than Pt(0) but the differences were small. Although the catalytic activity of rutile was much less than that of the P25, the effect of platinum addition was so much greater on rutile than on P25 that the activities of the Pt treated titanias were similar. Charge carrier separation by platinum is probably much more significant on rutile than on P25.

Neither the platinum-free catalysts nor any of the Pt/P25 catalysts oxidized DCA when excited by ‘visible’ radiation ($\lambda_{\text{max}} = 435$ and 490 nm). However, ‘visible’ light irradiation of Pt/rutile did oxidize DCA. Visible light photocatalysis by Pt/rutile was over three times faster than UV photocatalysis by untreated rutile powder. This suggests that electron trapping by Pt/rutile allows effective utilization of the small 405 nm component emitted by ‘visible’ radiation sources.

© 2007 Elsevier B.V. All rights reserved.

Keywords: Titanium dioxide; Rutile; Anatase; Photocatalysis; UV; Visible photocatalysis; Dichloroacetic acid

1. Introduction

The application of TiO_2 for photocatalytic oxidation of organic molecules [1–3] is limited by both high charge carrier recombination rates [4] and, usually, the need for ultraviolet excitation. Platinum, and other noble metals, may decrease charge carrier recombination, when deposited on the TiO_2 surface, by providing an electron sink [5], and have been proposed to extend the absorption of the catalyst into the visible portion of the spectrum [6–9]. On P25, platinum addition increased dichloroacetic acid (DCA) and trichloroacetic acid (TCA) oxidation rates by a factor of 2–3 [10–12]. Chloroform reduction was decreased [13] and trichloroethylene (TCE) degradation rates were generally decreased as well [12–14]. Dichloropropionic acid (DCP) oxidation was increased by a factor of only 1.5 [13].

Variations in platinum loading, oxidation state and the nature of the catalysed reaction all influence the results. The influence of the TiO_2 has been compared less often, although the effects of anatase area and crystallinity [10] and of anatase–rutile composition (varied by preferential HF-dissolution of the anatase component in P25) [11] on the activity of Pt/ TiO_2 have been studied. 0.2 wt% Pt(0) on rutile was reported to increase oxidation rates by a factor of 7.5 [11]. In addition, Ag/anatase and Ag/rutile [15] and Pt/Ag/anatase and Pt/Ag/rutile have been compared [16]. This aspect, the influence of TiO_2 type, is the focus of this paper.

The oxidation of dichloroacetic acid (DCA), a reaction that has previously been reported to be sensitive to the presence of platinum, was used to probe the differences between platinisation of Degussa P25 and of nano-particulate rutile. A pH of 3 was chosen to maximize adsorption of the negatively charged dichloroacetate ion (the main species in solutions of DCA at pH 3), on the titania, which is positively charged at this pH. At higher pHs, near the isoelectric point ($\text{pH} \sim 6$) of the TiO_2 , the adsorption of the negatively charged anion would change rapidly as the surface charge on the titania changes. By

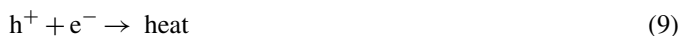
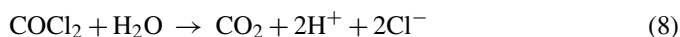
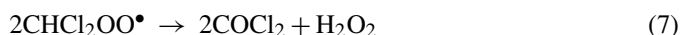
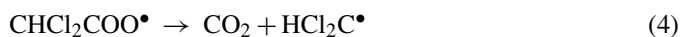
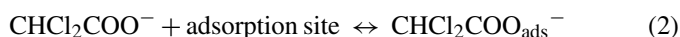
* Corresponding author at: School of Chemical Engineering & Advanced Materials, Bedson Building, University of Newcastle Upon Tyne, Newcastle Upon Tyne NE1 7RU, UK. Tel.: +44 191 222 5618.

E-mail address: T.A.Egerton@ncl.ac.uk (T.A. Egerton).

carrying out experiments at pH 3 such fluctuations in the amount of adsorption were minimized.

Because of previous reports that the Pt oxidation state may influence oxidation of chloro-compounds [12] the Pt oxidation state has been deliberately varied.

The primary step of photodegradation of DCA is generally considered [17] to be oxidation by direct transfer of photogenerated holes. A proposed reaction scheme [18] is



According to this mechanism, oxygen acts as an electron scavenger, thus optimising electron–hole separation and also plays a role in the degradation of one of the intermediates (reaction (6)). Kim and Choi [11] recognized that O_2 also acts as an electron scavenger during trichloroacetate degradation to Cl^- , and that in its absence an alternative path, leading to DCA formation is favoured.

2. Experimental

2.1. Materials

Degussa P25, a $\sim 50 \text{ m}^2 \text{ g}^{-1}$, 80:20 anatase:rutile powder, was used as received. The $\sim 120 \text{ m}^2 \text{ g}^{-1}$ rutile sample (HAR3), prepared by hydrolysis of TiCl_4 was supplied by Dr. I. Tooley of Uniqema (now Croda) UK. The platinum precursor was K_2PtCl_6 (Fluka, 40 wt% Pt). Dichloroacetic acid (Alfa Aesar, 99%), sodium nitrate and sodium hydroxide (both Riedel de Haen, puriss) were used as received from the suppliers.

2.2. Preparation and characterization of TiO_2/Pt catalysts

Appropriate amounts of platinum precursor were dissolved in water and TiO_2 was added to make a 10 g dm^{-3} slurry whose pH was adjusted to either 3 or 10, in accordance with established methods [19]. The platinum was photodeposited on the suspension of TiO_2 by irradiation for 3 h, using a Philips PL-L 36W 09 actinic lamp placed in the centre of the reaction vessel, and

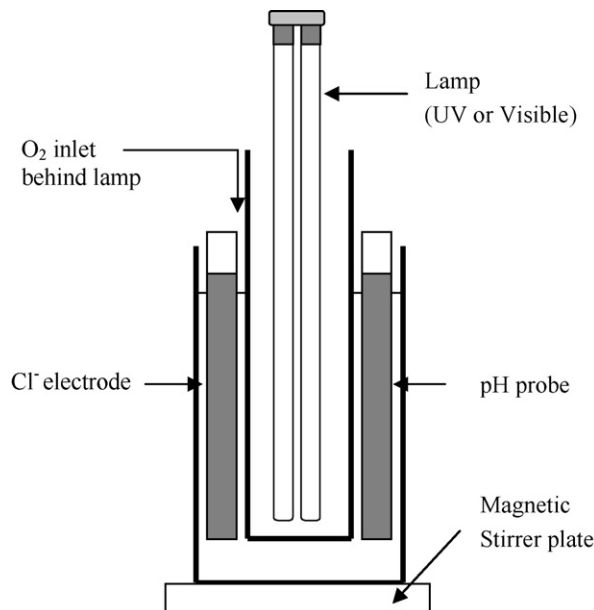


Fig. 1. Reaction set-up for DCA oxidation experiments.

then filtered. The resulting powder was thoroughly washed (to a filtrate conductivity of $<200 \mu\text{S}$) and dried at 160°C for 16 h. Solutions were analysed by inductively coupled plasma spectroscopy (Unicam 701 ICP-OES) before and after irradiation and the final platinum loading on the TiO_2 was determined by mass balance. XPS measurements were performed using an ESCA 300 photoelectron spectrometer. Samples were mounted on a stainless steel holder and irradiated with a flood gun (7–8 eV) to compensate for charging effects. Pt 4f, Ti 2p and O 1s spectra were measured using monochromated Al $\text{K}\alpha$ radiation and the O 1s line was used to calibrate the Pt 4f binding energies.

2.3. DCA photooxidation measurements

Oxidation of dichloroacetate ions was carried out with a loading of 1 g of catalyst in 250 ml of 36 mM DCA. Two milliliters of 5 M NaNO_3 was added to adjust the ionic strength (to $\sim 40 \text{ mM}$) to ensure that the electrode response was not unduly affected by minor changes in electrolyte concentration. One molar NaOH was added to adjust the pH to 3 (as its pK_a is 1.29, DCA is predominantly in its ionized form at pH 3). Prior to irradiation, dispersions were stirred using a magnetic stirring bar for 30 min with a constant flow of oxygen. For the UV photocatalysis, the suspension was then irradiated by a Philips PL-L 36W 09 actinic lamp, with a peak UV intensity at $\sim 360 \text{ nm}$, placed in an axial well within the reactor (as shown in Fig. 1). For photocatalysis by visible light, the suspension was irradiated by a Sylvania CF-L 36W lamp with output $>400 \text{ nm}$ (peak outputs are at 435 and 490 nm). Although this light emits primarily in the visible, the lower edge of its emission is at 405 nm. The outputs of these two lamps, measured immediately outside the empty reactor using a Bentham spectroradiometer, are compared in Fig. 2. The photoactivity of all samples was measured by monitoring the generation of chloride ions from the oxidation of DCA (Eq.

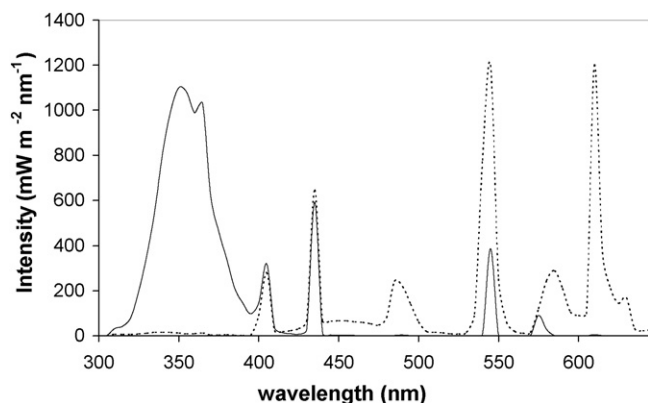


Fig. 2. Intensity of radiation from lamps used: UV lamp (—); 'visible' lamp (---). The radiometer detector was positioned against the outer wall of the reactor with the lamps being inside the well within the reactor (see Fig. 1).

(8)) using a chloride ion selective electrode. Zero-order kinetics were observed in all cases.

3. Results

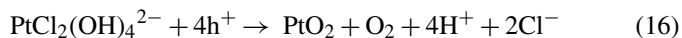
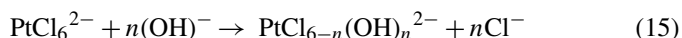
3.1. Characterization of the Pt/TiO₂ catalysts

A pH of 3 was chosen for photo-deposition of Pt because, as suggested by Zhang et al. [19], at pH 3 the platinum complex exists as the hexa-chloride ion and by accepting four photo-generated electrons deposits according to the following equation:

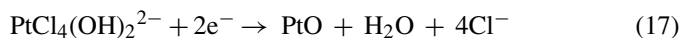


Similarly previous studies have suggested [19] that at pH 10, in the presence of photogenerated holes, the largely hydroxylated platinum complex ($2 < n < 6$) can deposit onto the titania surface in a high oxidation state according to Eq. (16) or accept two

electrons as in Eq. (17):



or



As the surface area ($\sim 120 \text{ m}^2 \text{ g}^{-1}$) of the rutile used in our studies is significantly larger than that of P25 ($50 \text{ m}^2 \text{ g}^{-1}$) the Pt loadings of 0.38 wt% (HAR3) and 0.15 wt% (P25) were selected in order to give comparable surface coverages. High area rutile, samples with 0.38, 0.7 and 1 wt% Pt(II) and P25 samples with 0.15 and 0.38 wt% Pt(II) were made. In order to compare the effects of platinum oxidation state, a rutile with 0.38 wt% Pt(0) and a P25 with 0.15 wt% Pt(0) were also made.

Catalysts prepared at high pH were greenish, those prepared at low pH were grey, suggesting that different oxidation states had been achieved. XPS measurements for the high pH samples gave peaks with binding energies of 72.85 and 76.13 eV, consistent with published values [20] for Pt(II). Spectra of the low pH samples gave binding energies of 70.5 and 73.86 eV, consistent with published values [20] for Pt(0).

TEM images of Pt(II) on P25 and rutile are shown in Fig. 3a and b which clearly demonstrate the different morphologies of the two titanias. The presence of platinum is much less obvious on the rutile than on the P25, suggesting that platinum may be smaller on rutile than on the predominantly anatase P25. For rutile the Pt crystallite size is of the order of 7 nm and 14 nm for anatase. (Because the platinum loading is very low few Pt particles are seen in any one micrograph and a more accurate measurement of platinum size distribution would require sizing of many particles.) Sarukawa and Matsumura [21] have reported that deposition of Pt, from PtCl_6^{2-} , on a mixture of rutile and anatase $1 \mu\text{m}$ crystals was mainly on the $\{110\}$ face of the rutile crystals. Since the $\{110\}$ faces are dominant in the needle

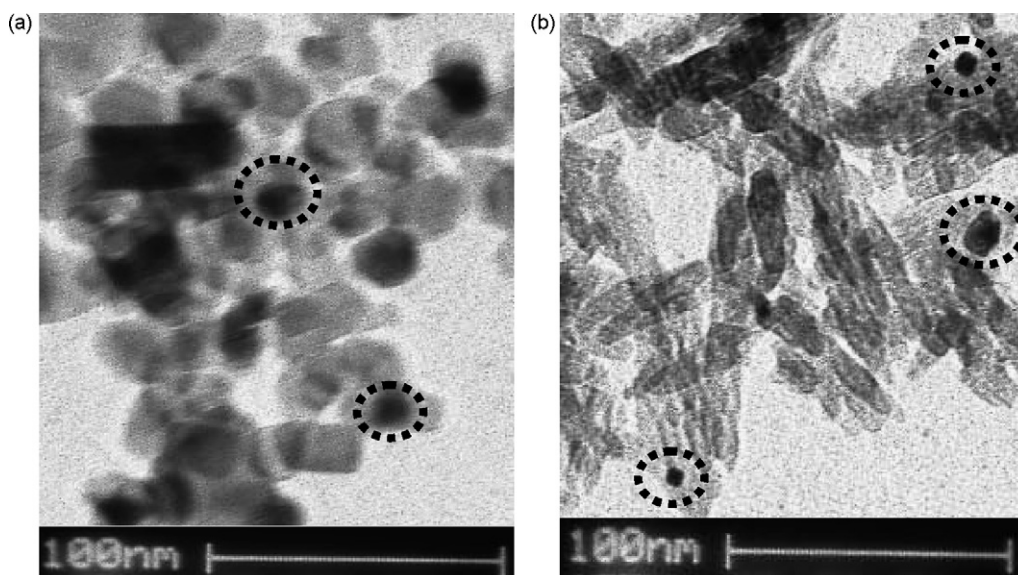


Fig. 3. TEM images of Pt(II) on (a) P25 (left) and (b) rutile (right). The dashed circles highlight selected Pt particles.

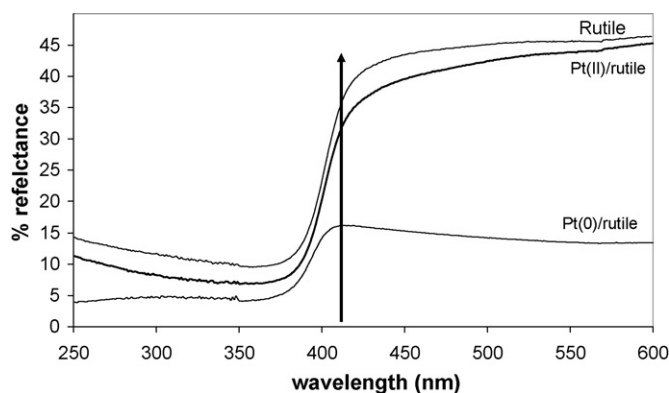


Fig. 4. Reflectance spectra of untreated rutile, Pt(II)/rutile and Pt(0)/rutile. The arrow is at ~ 410 nm (i.e. the absorption edge of rutile).

shaped rutile (Fig. 3b), we speculate that the ready deposition of Pt on this face leads to many, small, Pt crystallites whereas the less facile deposition on anatase leads to fewer Pt nuclei and correspondingly larger particles. Representative reflectance spectra of these Pt added rutile samples are shown in Fig. 4. Although the Pt deposition changes the visible reflectance there is no sign of a shift in the TiO_2 absorption edge. Nor was any shift observed in the transmission spectra (not shown) of the catalyst dispersions.

3.2. UV photocatalysis of DCA oxidation by P25 and rutile

Preliminary experiments confirmed that no DCA oxidation occurred in the absence of TiO_2 and that no photogeneration of Cl^- from the Pt treated catalyst occurs in the absence of DCA. The rates of photocatalytic chloride ion generation by P25 and rutile are compared in Fig. 5 which shows the (15 \times) higher activity of the P25.

Fig. 6 shows that on P25 ($50 \text{ m}^2 \text{ g}^{-1}$) the effects of deposited platinum on the same reaction were relatively small. The rate increased by a factor of 1.6 for 0.15% Pt(II) (chosen to give a Pt surface coverage comparable with that of the 0.38% Pt on the $\sim 120 \text{ m}^2 \text{ g}^{-1}$ rutile) and by 1.5 for 0.38% Pt(II). Deposition of 0.15% Pt(0) slightly decreased the activity by 25%. By comparison, Hufschmidt et al. [10] reported photonic efficiencies

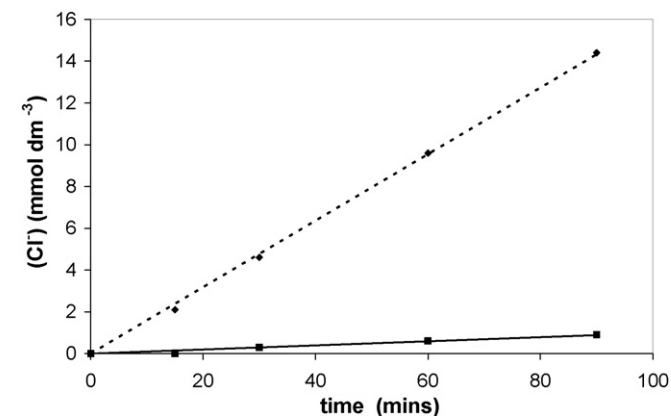


Fig. 5. UV photocatalysed Cl^- generation at pH 3 with P25 (---, \blacklozenge) and rutile (—, \blacksquare).

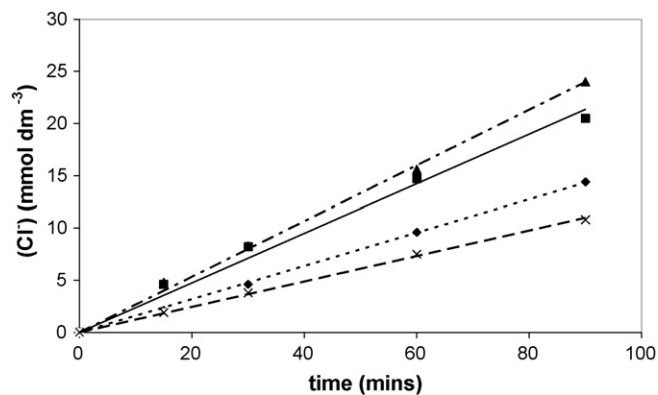


Fig. 6. UV photocatalysed Cl^- generation on Pt/P25 catalysts: P25 (---, \blacklozenge); P25/0.15 wt% Pt(II) (---, \blacktriangle); P25/0.38 wt% Pt(II) (—, \blacksquare); P25/0.15 wt% Pt(0) (---, \times).

increased by a factor of 2.6 for 0.5% Pt, and 2.2 for 1% Pt at pH 3, although it is not clear what the platinum oxidation state was in these cases.

By contrast (Fig. 7), 0.38 wt% platinum addition to rutile increased the activity for DCA oxidation by 3300% for Pt(0) and 3750% for Pt(II). Increasing the Pt(II) loading from 0.38 to 0.7 to 1 wt%, progressively decreased the DCA oxidation activity, analogous to the report of Hufschmidt et al. [10]. However, the decreases were small compared to the overall positive effect of the platinum. It is significant that although the effect of Pt on the rutile was so much larger than on P25 the highest rates achieved were similar in the two cases. The rates for all samples are summarised in Table 1.

Beneficial effects of platinum on rutile have also been observed in studies of azo dye decolouration and of propan-2-ol oxidation. The magnitude of the effects varies with the system being studied and a detailed analysis is currently in preparation.

3.3. Visible light photocatalysis of DCA oxidation by P25 and rutile

The results in Fig. 8 show that, although the high area rutile is active for dichloroacetate (DCA) oxidation under UV irradiation, it has negligible activity under 'visible' light irradiation.

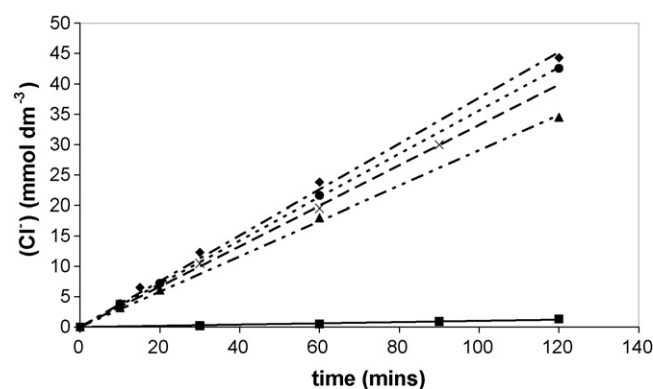


Fig. 7. UV photocatalysed Cl^- generation on rutile catalysts: rutile (—, \blacksquare); rutile/0.38 wt% Pt(II) (---, \blacklozenge); rutile/0.7 wt% Pt(II) (---, \bullet); rutile/1 wt% Pt(II) (---, \blacktriangle); rutile/0.38 wt% Pt(0) (---, \times).

Table 1

Table showing absolute chloride generation (after 1 h) and relative rate constants (rate constants are per unit area of catalyst) for UV photocatalysis

Sample	[Cl ⁻] at 60 min mM ⁻¹	Rate constant (mM min ⁻¹ m ⁻²)	Enhancement factor
Rutile	0.6	8.42×10^{-5}	–
Rutile/0.38 wt% Pt(II)	24	3.14×10^{-3}	37
Rutile/0.7 wt% Pt(II)	22	2.97×10^{-3}	35
Rutile/1 wt% Pt(II)	18	2.42×10^{-3}	29
Rutile/0.38 wt% Pt(0)	20	2.77×10^{-3}	33
P25	9.6	3.18×10^{-3}	–
P25/0.15 wt% Pt(II)	16	5.32×10^{-3}	1.7
P25/0.38 wt% Pt(II)	15	4.74×10^{-3}	1.5
P25/0.15 wt% Pt(0)	7.5	2.44×10^{-3}	0.8

However, when the 0.38% Pt(II) or Pt(0) on rutile catalyst was irradiated with visible light, there was significant DCA degradation. The ‘visible’ light photocatalytic activity of Pt(0)/rutile was comparable with, albeit a little lower, than that of its higher oxidation state equivalent. Remarkably, the Pt added catalysts oxidized DCA over three times faster with visible light, than the untreated rutile powder did when UV irradiated.

In clear contrast the addition of 0.38 wt% Pt(II) to Degussa P25 does not increase the rate of visible light oxidation. Platinised P25 showed only ~6% of the activity of the rutile equivalent.

4. Discussion

4.1. Photocatalysis by P25 and rutile

The two titania samples that have been studied were a high area (120 m² g⁻¹) pure rutile, composed of elongated particles and Degussa P25, an 80 m² g⁻¹ mixture of (mainly) anatase and rutile composed of practically spherical particles. The differences in the surface area and shape may affect the distribution of the platinum particles on the two titanias. However, this discussion focuses on the different roles of the anatase and rutile. The reasons for the greater activity of anatase have been widely debated in the literature. Following others [22,23], we

consider, that an important reason is that O₂^{•-} formation on anatase is easier as a consequence of the higher energy (by ~0.2 eV) of its conduction band relative to that of rutile. In turn, this more rapid transfer of electrons to O₂ reduces surface electron–hole recombination and increases the photocatalytic activity. In addition, it has been suggested that photocatalytic activity of Degussa P25 is enhanced by additional charge separation resulting from the presence of both rutile and anatase phases. Conventionally, it is proposed that, because the rutile phase acts as an electron sink for anatase, electron–hole separation is increased [24] though recent EPR studies [25] conclude that it is deep trap levels in the anatase of P25 that act as the electron sink.

Enriquez et al. have recently suggested [26] that the role of adsorption is particularly important for photocatalysis of molecules, such as DCA in which oxidation occurs by direct hole transfer. However, the possibility that the greater DCA oxidation on the untreated anatase is due to differences in adsorption is excluded because our direct measurements showed adsorption per unit area to be similar on the two titanias even though the adsorption per unit weight was greater on rutile.

4.2. UV photocatalysis by Pt/P25 and Pt/rutile

Platinum addition affected the photocatalytic activity of both catalysts. The results were generally consistent with the view that, because the Fermi energy of Pt is initially lower than that of the TiO₂, electrons generated during band gap irradiation move to the Pt and hence reduce the recombination (Eq. (9)) which would otherwise decrease the concentration of the holes that oxidize the DCA anions (Eq. (3)). If, as has also been suggested [27], an electrostatic layer composed of negatively charged Pt particles is formed it will attract positive holes to the TiO₂ surface whilst driving electrons into the bulk. This effect, analogous to the electric field enhancement effect in photoelectrocatalysis [28], will also decrease recombination and enhance photocatalytic activity.

As outlined in Section 4.1, the surface recombination in P25 is less important than in rutile because of more effective charge separation, since adsorbed oxygen is more able to capture electrons from the anatase conduction band and/or additional charge separation in P25. When Pt is present on the surface, it too captures electrons from the conduction band. However, because of the existing charge separation mechanism on P25, the additional improvement induced by Pt is small. On rutile, however, even though oxygen is relatively ineffective at trapping electrons from the conduction band, the platinum is able to trap them efficiently (it has been suggested that the work function of Pt is 0.3 eV more than that of the sputter-annealed TiO₂ surface) [27]. Consequently Pt makes a much greater difference to rutile than it does to anatase. However, although the difference induced by Pt is much greater for rutile than for P25, the optimum rate constants for the two systems, 3.1 and 5.3 × 10⁻³ mM min⁻¹ m⁻², for rutile and P25, respectively, imply that the combination of intrinsic and Pt-induced charge separation on the Pt/TiO₂ samples are similar.

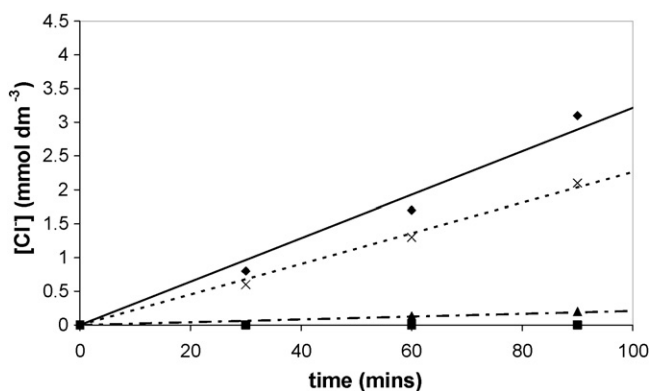


Fig. 8. Visible radiation photocatalysed Cl⁻ generation for various catalysts: rutile (—, ■); rutile/0.38 wt% Pt(II) (—, ◆); rutile/0.38 wt% Pt(0) (---, ×); P25/0.38 wt% Pt(II) (- - -, ▲).

The primary effect of the platinum, charge separation of electrons and holes, could be influenced by differences in the platinum distribution on the surface of the two titanias. For a fixed weight of platinum, bigger particles result in fewer particles and the resulting greater diffusion distance of charge carriers to the platinum crystallites could lessen their effectiveness as electron traps. The ability to trap electrons may also be affected if the Fermi level is altered as a consequence of Pt crystal size changes. Although other effects, e.g. the proportion of low coordination sites on the platinum surface, also depend on the metal crystallite size [29] they are considered to be of lesser importance for photocatalytic reactions. Others have demonstrated that, for a given catalyst, increasing the platinum loading increases the number, not the size, of the particles [20]. (This is reasonable, since a simple calculation suggests that, for 0.38% Pt in the form of 7.5 nm hemispherical crystallites on $120 \text{ m}^2 \text{ g}^{-1}$ rutile, the number of Pt particles is <1% of the number of TiO_2 particles.) As we have shown (Fig. 7) that the changes of the platinum loading on rutile have only a small effect on photoactivity (compared to the overall increase) it is concluded that at the levels employed in this study, for which Pt–Pt distances are of the order of 200 nm, the number of platinum particles has only a secondary effect on their effectiveness as electron traps. Electron capture may involve diffusion across many TiO_2 particles—the ‘antenna effect’ described by Bahnemann et al. [30] The effect of metal crystallite size on Fermi level is, in principle, more complex. However, as 0.38 wt% platinum addition to rutile increased the activity for DCA oxidation by 3300% for Pt(0) and by 3750% for Pt(II) we conclude that the effect of Fermi level change is also likely to have only second order effects. This may be because, as shown by Mulvaney et al. [31], for zinc oxide (ZnO), platinum is a very effective electron sink—far more effective than gold. This could explain why size effects for platinum are less important than for gold for which smaller particles (3 nm) enhanced charge separation better than larger particles (8 nm) [32]. Even reduction of Au particle-size from 18 to 4 nm only increased the apparent rate constant for photocatalytic destruction of oxalic acid by a factor of 2 [33].

4.3. The effect of Pt oxidation state and loading on the UV photocatalysis

For both P25 and rutile our results demonstrate that platinum in the (mainly) 2+ oxidized state is better for DCA oxidation than reduced platinum metal. This result is consistent with a previous study by Yang et al. [34], where they showed the quantum yield of DCA decomposition decreased when Pt(II/IV) on Hombikat anatase was reduced to Pt(0). Reduction of the platinum will raise the Fermi level and hence make the Pt sink less effective.

For both rutile and P25, increased platinum loading resulted in a small decrease in oxidation rate (see Table 1). Since, the decrease was small in comparison with the overall effect of the platinum, the effect was only measured with oxidized platinum materials. The levels of platinum were sufficiently low to exclude the ‘shadowing’ effects that have been suggested to explain decreases in rate with increasing levels of either silver or platinum [35]. It is possible that platinum is photodeposited

on, and therefore quenches, photocatalytic sites and this would lead to the observed dependence on the base TiO_2 material.

4.4. Visible photocatalysis by Pt/P25 and Pt/rutile

As expected, neither the platinum-free catalysts nor any of the Pt/P25 catalysts oxidized DCA when excited by ‘visible’ radiation. Remarkably, visible light irradiation of the 0.38% Pt/rutile oxidized DCA over three times faster than UV irradiation of untreated rutile powder.

Visible light activity of N doped [36], C doped [37] and S doped [38] TiO_2 ’s is normally attributed to an extension of the TiO_2 absorption into the visible as a result of introducing localized levels which do not act as recombination centres. Pt/ TiO_2 materials can also act as visible light photocatalysts. Kisch has postulated that when platinum is incorporated into the TiO_2 lattice [39] (by sol–gel preparation) or when it is present as PtCl_4 ground into TiO_2 [40] a photo-excited electron from platinum can transfer into the conduction band of TiO_2 thus increasing the activity in a similar way to dye sensitisation, in which the TiO_2 acts, not as an intrinsic photocatalyst, but as an acceptor of electrons, which then initiate further reaction, from the photo-excited dye.

Since the Pt/rutile samples are coloured they must absorb in the visible. However, neither reflectance spectra (Fig. 4) nor careful transmission studies of light attenuation gave evidence that the addition of Pt had resulted in the TiO_2 absorption edge being extended into the visible portion of the spectrum. It therefore seems unlikely that the degradation induced by irradiation from the visible lamp is caused by changes in the TiO_2 band structure. Instead, we propose that the high activity of the Pt treated rutile is associated with the very small proportion of light emitted between 400 and 410 nm. This radiation does not cause excitation across the anatase band gap—for which the absorption edge is ~ 385 nm. For the rutile, however, the 405 nm radiation does cause excitation across the band gap and can be surprisingly effective. For propan-2-ol photocatalysis, when allowance is made for the dependence of rate on $I^{0.5}$, the photonic efficiency of the 405 nm emission of a medium pressure mercury arc lamp is approximately half of that of the 365 nm emission [41]. However, because the overall photonic efficiency of rutile is generally small, the rutile catalysts have negligible visible activity—as shown in Fig. 8. However, in our experiments Pt addition increased the overall activity of the rutile by a factor of ~ 35 . The consequence is that the activity induced by the radiation in the 400–410 nm range is also increased by a similar factor. Therefore, we propose that the ‘visible activity’ observed in our experiments is a consequence of the efficient utilization of the small number of photons at ~ 405 nm and that the efficiency gains caused by the presence of platinum amplify an effect which is normally ignored.

The implication of this result is that a significant response to wavelengths of ~ 400 – 410 nm can be expected in any rutile particles if they are modified in such a way as to reduce charge carrier recombination. It is important to differentiate between this effect and increases in activity caused by extending the absorption of radiation beyond the rutile absorption edge.

5. Conclusions

Although rutile is much less effective than P25 for the UV photocatalytic oxidation of DCA, Pt treatment enhances its activity to a level that is comparable with that of Pt on P25. This is attributed to electron trapping by the platinum on rutile being much more significant than for platinum on P25, for which alternative charge separation mechanisms exist.

This electron trapping enables platinum on rutile to effectively use the small amount of 405 nm radiation emitted by the ‘visible’ source. Although this radiation is also used by Pt-free rutile, it is then a small fraction of the already low activity of the Pt-free catalyst.

Acknowledgements

We are grateful to Uniqema (Dr. I. Tooley) for financial support via an EPSRC CASE award (JAM), also for the provision of the high area rutile sample and many helpful discussions. We thank Dr. L. Siller (Newcastle U.) for the measurement of the XPS spectra and Ms. M.A. Velazco-Roa for the reflectance spectra.

References

- [1] A. Wold, *Chem. Mater.* 5 (1993) 280–283.
- [2] M.R. Hoffmann, S.T. Martin, W. Choi, D.W. Bahnemann, *Chem. Rev.* 95 (1995) 69–96.
- [3] T.-H. Bui, M. Karkmaz, E. Puzenat, C. Guillard, J.-M. Herrmann, *Res. Chem. Intermed.* 33 (2007) 421–431.
- [4] L. Sun, J.R. Bolton, *J. Phys. Chem.* 100 (1996) 4127–4134.
- [5] B. Sun, A.V. Voronstov, P.G. Smirniotis, *Langmuir* 19 (2003) 3151–3156.
- [6] S. Kim, S.-J. Hwang, W. Choi, *J. Phys. Chem. B* 109 (2005) 24260–24267.
- [7] L. Zang, C. Lange, I. Abraham, S. Storck, W.F. Maier, H. Kisch, *J. Phys. Chem. B* 102 (1998) 10765–10771.
- [8] B. Sun, P.G. Smirniotis, P. Boolchand, *Langmuir* 21 (2005) 11397–11403.
- [9] W. Zhao, C. Chen, W. Ma, J. Zhao, D. Wang, H. Hidaka, N. Serpone, *Chem. Eur. J.* 9 (2003) 3292–3299.
- [10] D. Hufschmidt, D. Bahnemann, J.J. Testa, C.A. Emilio, M.I. Litter, *J. Photochem. Photobiol. A: Chem.* 148 (2002) 223–231.
- [11] S. Kim, W. Choi, *J. Phys. Chem. B* 106 (2002) 13311–13317.
- [12] J. Lee, W. Choi, *J. Phys. Chem. B* 109 (2005) 7399–7406.
- [13] J. Chen, D.F. Ollis, W.H. Rulkens, H. Bruning, *Water Res.* 33 (1999) 661–668.
- [14] M.D. Driessen, V.H. Grassian, *J. Phys. Chem. B* 102 (1998) 1418–1423.
- [15] A. Sclafani, M.-N. Mozzanega, J.-M. Herrmann, *J. Catal.* 168 (1997) 117–120.
- [16] A. Sclafani, J.-M. Herrmann, *J. Photochem. Photobiol. A: Chem.* 113 (1998) 181–188.
- [17] D.W. Bahnemann, M. Hilgendorff, R. Memming, *J. Phys. Chem. B* 101 (1997) 4265–4275.
- [18] C.S. Zalazar, R.L. Romero, C.A. Martin, A.E. Cassano, *Chem. Eng. Sci.* 60 (2005) 5240–5454.
- [19] F. Zhang, J. Chen, X. Zhang, W. Gao, R. Jin, N. Guan, Y. Li, *Langmuir* 20 (2004) 9329–9334.
- [20] B. Ohtani, K. Iwai, S. Mishimoto, S. Sato, *J. Phys. Chem. B* 101 (1997) 3349–3359.
- [21] T. Ohno, K. Sarukawa, M. Matsumura, *N. J. Chem.* 26 (2002) 1167–1170.
- [22] A. Mills, S. Le Hunte, *J. Photochem. Photobiol. A: Chem.* 108 (1997) 1–35.
- [23] O. Carp, C.L. Huisman, A. Reller, *Prog. Solid State Chem.* 32 (2004) 33–177.
- [24] R.I. Bickley, T. Gonzalez-Carreno, J.S. Lees, L. Palmisano, R.J.D. Tilley, *J. Solid State Chem.* 92 (1991) 178–190.
- [25] D.C. Hurum, A.G. Agrios, K.A. Gray, T. Rajh, M.C. Thurnauer, *J. Phys. Chem. B* 107 (2003) 4545–4549.
- [26] R. Enriquez, A.G. Agrios, P. Pichat, *Catal. Today* 120 (2007) 196–202.
- [27] H. Uetsuka, C. Pang, A. Sasahara, H. Onishi, *Langmuir* 21 (2005) 11802–11805.
- [28] K. Vindogopal, U. Stafford, K.A. Gray, P.V. Kamat, *J. Phys. Chem.* 98 (1994) 6797–6803.
- [29] R. Van Hardeveld, A. van Montfoort, *Surf. Sci.* 4 (1966) 396.
- [30] C. Wang, R. Pagel, J.K. Dohrmann, D.W. Bahnemann, C.R. Chim. 9 (2006) 761–773.
- [31] A. Wood, M. Giersig, P. Mulvaney, *J. Phys. Chem. B* 105 (2001) 8810–8815.
- [32] V. Subramanian, E.E. Wolf, P.V. Kamat, *J. Am. Chem. Soc.* 126 (2004) 4943–4950.
- [33] V. Iliev, D. Tomova, L. Bilyarska, G. Tyuliev, *J. Mol. Catal. A: Chem.* 263 (2007) 32–38.
- [34] J.C. Yang, Y.C. Kim, Y.G. Shul, C.H. Shin, T.K. Lee, *Appl. Surf. Sci.* 121/122 (1997) 525–529.
- [35] M. Huang, E. Tso, A.K. Datye, M.R. Prairie, B.M. Stange, *Environ. Sci. Technol.* 30 (1996) 3084–3088.
- [36] R. Asahi, T. Morikawa, T. Ohwaki, K. Aoki, Y. Taga, *Science* 293 (2001) 269–271.
- [37] S. Sakthivel, H. Kisch, *Angew. Chem. Int. Ed.* 42 (2003) 4908–4911.
- [38] R. Bacsa, J. Kiwi, T. Ohno, P. Albers, V. Nadtochenko, *J. Phys. Chem. B* 109 (2005) 5994–6003.
- [39] L. Zang, C. Lange, I. Abraham, S. Storck, W.F. Maier, H. Kisch, *J. Phys. Chem.* 102 (1998) 10765–10771.
- [40] W. Macyk, H. Kisch, *Chem. Eur. J.* 7 (2001) 1862–1867.
- [41] T.A. Egerton, C.J. King, *J. Oil Colour Chem. Assoc.* 62 (1979) 386–391.